

Received April 04, 2019; reviewed; accepted May 08, 2019

## Influencing mechanisms of sodium hexametaphosphate on molybdenite flotation using sea water

Lizhangzheng Wang <sup>1</sup>, Yubiao Li <sup>1,2</sup>, Ruihua Fan <sup>1</sup>, Rong Fan <sup>3</sup>

<sup>1</sup> School of Resources and Environmental Engineering, Wuhan University of Technology, Wuhan, 430070, China

<sup>2</sup> Hubei Key Laboratory of Mineral Resources Processing & Environment, Wuhan 430070, China

<sup>3</sup> CSIRO Mineral Resources, Private Bag 10, Clayton South, VIC, 3169, Australia

Corresponding author: Yubiao.Li@whut.edu.cn (Y. Li)

**Abstract:** Flotation using sea water has been considered as a promising alternative to concentrate molybdenite (MoS<sub>2</sub>) under alkaline conditions due to scarcity of fresh water and increasingly strict regulations on the quality of discharged water. However, the MoS<sub>2</sub> recovery with sea water during flotation has not been satisfactory, owing to the depressing effects from the hydrophilic metallic species onto MoS<sub>2</sub> surface. This study combines experimental and theoretical studies of MoS<sub>2</sub> flotation to investigate how the physicochemical properties of MoS<sub>2</sub> vary with the addition of a dispersant, sodium hexametaphosphate (SHMP), and in sea and fresh water. Our experimental results show that the addition of SHMP during flotation has increased the recovery of MoS<sub>2</sub>, via reducing the adsorption of the hydrophilic metallic precipitation onto MoS<sub>2</sub> surface. The DLVO calculation confirms that the addition of SHMP increases the floatability of MoS<sub>2</sub> by dispersing the formed hydrophilic metallic precipitation (Mg(OH)<sub>2</sub> colloids) from the MoS<sub>2</sub> surface, via reversing attraction force to repulsion force, thereby improving MoS<sub>2</sub> flotation recovery.

**Keywords:** sodium hexametaphosphate, flotation, molybdenite, sea water, mechanism

### 1. Introduction

Molybdenite (MoS<sub>2</sub>), the largest source of molybdenum (Mo) on the Earth, with approximately half of the Mo being beneficiated from the Cu-Mo ores via flotation process (Liu, 2012). Water, primarily fresh water, is essential to various steps of the flotation process and the water use could be quite high. Due to the increasing scarcity of fresh water and increasingly strict regulations on the quality of discharged water, more processing operations utilised sea water as an alternative water resource for mineral flotation (Wang and Peng, 2014), especially for those sited in the sea water-abundant area, *e.g.*, in Chile, Australia (Arias et al., 2017; Li et al., 2018).

However, many previous studies show that the use of sea water reduces MoS<sub>2</sub> floatability under high alkaline condition (Qiu et al., 2016; Ramos et al., 2013; Rebolledo et al., 2017; Suyantara et al., 2018). For instance, Ramos et al. (2013) reported that the decreased MoS<sub>2</sub> recovery was mainly due to the adsorption of hydrophilic Mg species formed on the MoS<sub>2</sub> surface. Qiu et al. (2016) found that both Mg(OH)<sub>2</sub> and CaCO<sub>3</sub> were formed on MoS<sub>2</sub> surface, reducing the hydrophobicity and floatability of MoS<sub>2</sub>. In those studies, the precipitation on MoS<sub>2</sub> surface contributed to the hydrophobic surface.

Sodium hexametaphosphate ((NaPO<sub>3</sub>)<sub>6</sub>, SHMP) is normally used as a dispersant in mineral flotation, with the hydrogen phosphates as its effective component in solution (Lu et al., 2019). Li et al. (2017) found that SHMP can change the surface charge of serpentine and ascharite, thereby preventing the inter-particle agglomeration between minerals and particles. Rebolledo et al. (2017) investigated the possibility of MoS<sub>2</sub> flotation in sea water in the presence of SHMP. Recently, Li et al. (2018) reported that the addition of SHMP can reduce the adsorption of precipitation on chalcopyrite surface. However, the mechanism has not been fully understood, especially in the sea water system.

The objective of the present study is to investigate how the physicochemical properties vary with and without SHMP in fresh and sea water. Both water type and the addition of SHMP can influence surface reactivity of MoS<sub>2</sub> and hence impact the flotation recovery. Flotation tests, as well as various measurements such as contact angle, zeta potential and XPS were thus carried out to better understand the influencing mechanisms of SHMP on MoS<sub>2</sub> flotation in sea water. In addition, DLVO theory was applied to calculate the forces between the formed species and MoS<sub>2</sub> surface.

## 2. Material and methods

### 2.1. Samples and reagents

The MoS<sub>2</sub> samples were sourced from Guilin city, Guangxi province of China. After crushing and grinding, the MoS<sub>2</sub> powders were wet sieved, a particle size of 38~75µm was used for flotation tests while the <38µm powders were prepared for zeta potential measurements. All analytical reagents were purchased from China Sinopharm Chemical Reagent Co., Ltd, e.g. sodium hydroxide (NaOH), hydrochloric acid (HCl), sodium chloride (NaCl), potassium chloride (KCl), calcium chloride (CaCl<sub>2</sub>), magnesium chloride hexahydrate (MgCl<sub>2</sub>·6H<sub>2</sub>O), sodium bicarbonate (NaHCO<sub>3</sub>), magnesium sulfate heptahydrate (MgSO<sub>4</sub>·7H<sub>2</sub>O) and potassium bromide (KBr).

### 2.2. Flotation experiments

The flotation tests were carried out in a XFG-type flotation machine (same to the Fig. 1 shown in Li and Li (2019)) made by Wuhan Exploration Machinery Factory (Wuhan, China). 0.25g of MoS<sub>2</sub> particles was added into the flotation cell filled with 25 mL solution. The composition of sea water is same to that reported in Qiu et al. (2016) and Li and Li (2019), including 0.47 NaCl, 0.01 M KCl, 0.01 CaCl<sub>2</sub>, 0.025 M MgCl<sub>2</sub>, 0.0018 M NaHCO<sub>3</sub>, 0.028 M MgSO<sub>4</sub> and 0.00087 M KBr. The flotation machine was operated at 1200 rpm and the pulp pH was controlled using NaOH or HCl at a desired value during the first 6 minutes. After introducing air (100 mL min<sup>-1</sup>), the froth product was collected every 10 s. Both the floated concentrates and tailings were filtered and air dried, and then weighed for the calculation of cumulative recovery.

### 2.3. Contact angle measurements

The fresh MoS<sub>2</sub> surface was obtained by peeling of the chunk sample using adhesive tape and bathed in solution for 10 minutes. After that, the MoS<sub>2</sub> surface was washed three times using ultrapure water. After air drying, the MoS<sub>2</sub> surfaces treated under different conditions were placed into a contact-angle measuring device (JC2000C, Shanghai Zhongchen Digital Technology, China). The contact angles of several different areas on the treated MoS<sub>2</sub> surface were measured and the average values were reported.

### 2.4. Zeta potential measurements

The <38 µm MoS<sub>2</sub> particles were further ground to <5 µm in the Planetary Ball Mill Machine (DECO-PBD-V-0.4L, Changsha, China). 0.05g of obtained MoS<sub>2</sub> powders was placed into 50 mL conditioned solution and stirred for 10 minutes. NaOH or HCl was subsequently applied to adjust the solution pH. Then the zeta potential of the prepared pulp was determined by a Nano-ZS90 zeta potential analyzer (Malvern Co., Ltd, Malvern, UK). The average zeta potentials of three times were reported herein.

### 2.5. XPS measurements

Thermo Fisher ESCALAB 250Xi spectrometer (Waltham, MA, USA) with an Al K<sub>α</sub> X-ray source was applied to determine the MoS<sub>2</sub> surfaces treated under the conditions same to those for flotation. XPS Peak 4.1 software was used for analysis (Li and Li, 2019).

### 2.6. EDLVO calculation

The extended Derjaguin-Landau-Verwey-Overbeek (EDLVO) theory was used to explain the interaction between MoS<sub>2</sub> particles and other particles, where the total interaction energies ( $V_T$ ) equals to the sum of the Van der Waals interaction ( $V_W$ ), the electrostatic interaction ( $V_E$ ), and steric hindrance

effects ( $V_{SR}$ ), as shown in Eq. 1:

$$V_T = V_W + V_E + V_{SR} \quad (1)$$

where  $V_W$  can be calculated according to Eq. 2 while  $A$  can be calculation based on Eq. 3:

$$V_W = -\frac{A}{6H} \left( \frac{R_1 R_2}{R_1 + R_2} \right) \quad (2)$$

$$A = (\sqrt{A_{11}} - \sqrt{A_{33}})(\sqrt{A_{22}} - \sqrt{A_{33}}) \quad (3)$$

where  $A_{11}$  and  $A_{33}$  are the Hamaker constants of  $\text{MoS}_2$  ( $9.38 \times 10^{-20} \text{J}$ ) (Li et al., 2018) and water ( $3.7 \times 10^{-20} \text{J}$ ).  $A_{22}$  is the Hamaker constant of  $\text{MgO}$  as the alternative to  $\text{Mg(OH)}_2$  due to its unavailability.  $V_E$  can be calculated by Eq.4:

$$V_E = \frac{\pi \epsilon_0 \epsilon_r R_1 R_2}{R_1 + R_2} (\psi_1^2 + \psi_2^2) \left\{ \frac{2\psi_1 \psi_2}{\psi_1^2 + \psi_2^2} \ln \left[ \frac{1 + \exp(-\kappa H)}{1 - \exp(-\kappa H)} \right] + \ln[1 - \exp(-2\kappa H)] \right\} \quad (4)$$

where  $\epsilon_0$  and  $\epsilon_r$  are the vacuum dielectric constant and relative vacuum dielectric constant ( $6.95 \times 10^{-10} \text{C}^2 \cdot \text{J}^{-1} \cdot \text{m}^{-1}$ ).  $\kappa$  ( $0.18 \text{nm}^{-1}$ ) is the debye-huckl parameter.  $\varphi_1$ ,  $\varphi_2$  are the surface potentials of  $\text{MoS}_2$  and  $\text{Mg(OH)}_2$  particles. Usually, the surface potential of particles is represented by the zeta potential. The steric hindrance interaction energy  $V_{SR}$  can be described by Eq. 5:

$$V_{SR} = \frac{4\pi R^2 \left( \frac{\delta - H}{2} \right)}{Z(R + \delta)} kT \ln \left( \frac{2\delta}{H} \right) \quad (5)$$

where  $R$  is the radius of particles.  $\delta$  ( $5.45 \text{nm}$ ) represents the thickness of adsorbed layer after addition of SHMP.  $Z$  ( $1.9 \times 10^{-16} \text{m}^2$ ) refers to the covering area of the macromolecules on the particle surface. In addition,  $k$  ( $1.381 \times 10^{-23} \text{J/K}$ ) is the Boltzmann constant.

### 3. Results and discussion

#### 3.1. Flotation

Fig. 1 shows the recovery of  $\text{MoS}_2$  in pure water and sea water at pH ranging from 4 to 12.  $\text{MoS}_2$  recovery in sea water was greater than that in pure water when the solution pH was lower than 8, indicating that sea water was beneficial to  $\text{MoS}_2$  floatability at  $\text{pH} < 8$ . However, the  $\text{MoS}_2$  recovery in pure water was greater than that in sea water when the pH was over 8. This suggests that the flotation of  $\text{MoS}_2$  in sea water was depressed significantly at strong alkaline condition, consistent with previous studies (Castro et al., 2016; Jeldres et al., 2017; Li et al., 2018; Qiu et al., 2016). For instance, Suyantara et al. (2018) reported that the apparently decreased  $\text{MoS}_2$  recovery in sea water was attributed to the formation of Ca and Mg precipitation on mineral surface when pH was higher than 9. However,  $\text{MoS}_2$  recovery was only slightly decreased with increased pH in pure water, indicating that pH played an insignificant role on the natural floatability of  $\text{MoS}_2$ . Most previous studies indicated that  $\text{MoS}_2$  flotation was conducted under alkaline conditions, e.g. pH 10, at which some metallic ions can be precipitated due to the low solubility (Luis et al., 2015; Suyantara et al., 2018). The precipitated species might adsorb onto the mineral surface, thereby decreasing the flotation recovery (Li et al., 2018; Li et al., 2018; Wangqing et al., 2017). Further investigation of the beneficial conditions for  $\text{MoS}_2$  flotation was conducted at a selected pH of 10, based on the rational that  $\text{MoS}_2$  flotation was significantly decreased in sea water under alkaline conditions.

Fig. 2 shows the  $\text{MoS}_2$  recovery in pure and sea water at pH 10, with and without SHMP (50 mg/L). It is obvious that the recovery of  $\text{MoS}_2$  in pure water was not increased with the SHMP addition, indicating that SHMP had negligible effects on the natural floatability of  $\text{MoS}_2$  in pure water. In contrast, the addition of SHMP significantly increased  $\text{MoS}_2$  recovery in sea water, achieving a high recovery of 95%, compared to only approximately 60% without SHMP. Moreover, the flotation rate of  $\text{MoS}_2$  in the first 5 min was faster than that in the latter 5 min. Therefore, SHMP can relieve the inhibition effects of sea water on  $\text{MoS}_2$  flotation under alkaline conditions, resulting in faster kinetics and higher recovery.

#### 3.2. Contact angle

A higher contact angle corresponds to a lower wettability of minerals (Lazghab et al., 2005), generally resulting in greater floatability (Xia, 2017). Fig. 3 shows the effects of pH on contact angle of  $\text{MoS}_2$  surface treated under different conditions. The contact angle of  $\text{MoS}_2$  was reduced slightly with increased pulp

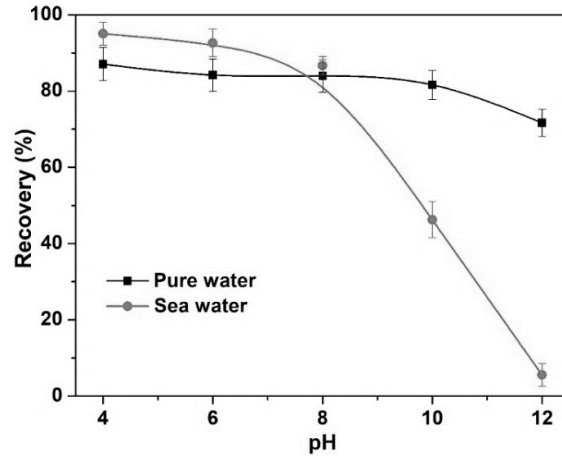


Fig. 1. MoS<sub>2</sub> recovery in pure water and sea water as a function of pH

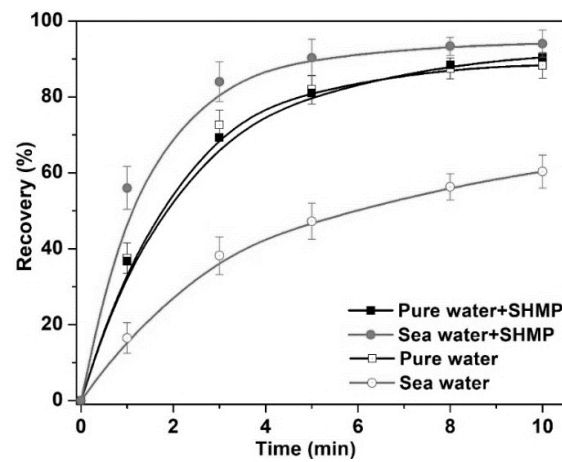


Fig. 2. MoS<sub>2</sub> recovery in pure water and sea water with/without 50 mg/L SHMP

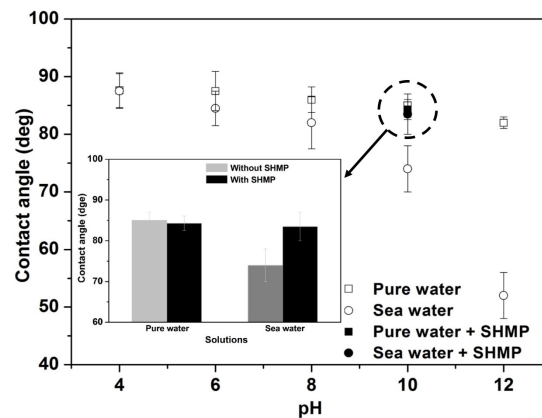


Fig. 3. Contact angle of MoS<sub>2</sub> treated in pure water and sea water

pH for pure water, suggesting that pH might play a negligible role on the hydrophobicity of MoS<sub>2</sub> surface. The presence of SHMP did not significantly change the contact angle of MoS<sub>2</sub> in pure water at pH 10, revealing that the addition of SHMP did not influence the natural wettability of MoS<sub>2</sub>, similar to that found for CuFeS<sub>2</sub> (Li and Li, 2019). However, the contact angle of MoS<sub>2</sub> surface was decreased in sea water with rising pH, showing that sea water adversely affected the hydrophobicity of MoS<sub>2</sub> surface. In addition, SHMP greatly increased the contact angle from 74° to 84° in sea water at pH 10, revealing that SHMP can relieve the decreased contact angle in sea water.

### 3.3. Zeta potential

Fig. 4 shows the zeta potential of  $\text{MoS}_2$  in pure water and sea water with and without SHMP within pH 4 ~ 12. The zeta potential of  $\text{MoS}_2$  in pure water was negative and gradually decreased with increased pH. Differently, the zeta potential of  $\text{MoS}_2$  in sea water was higher than that in pure water and increased with increasing pH. Specially, when  $\text{MoS}_2$  was treated in seawater, the zero electric point appeared at pH 9.2 where the zeta potential of  $\text{MoS}_2$  was reversed from negative to positive. These indicate that the positively charged metallic precipitation (hydrophilic) is adsorbed on the negatively charged  $\text{MoS}_2$  surface, thereby reducing  $\text{MoS}_2$  hydrophobicity and flotation recovery (Li et al., 2018).

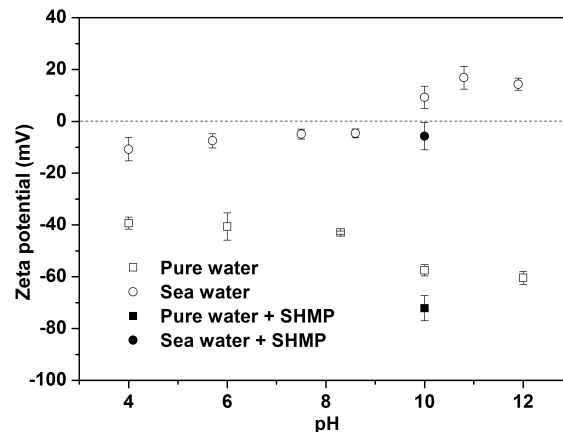


Fig. 4. Zeta potential of  $\text{MoS}_2$  in pure water and sea water as a function of pH

In addition, when SHMP was added at pH 10, the zeta potentials of  $\text{MoS}_2$  in both solutions were decreased and the zeta potential in sea water was even reversed from positive to negative again, indicating that the SHMP was capable of removing positively charged hydrophilic precipitation from  $\text{MoS}_2$  surface, presenting a cleaner surface for greater flotation recovery.

### 3.4. XPS analysis

Fig. 5 shows the XPS measurements of  $\text{MoS}_2$  surfaces treated under different conditions. Comparing to the untreated  $\text{MoS}_2$  (Fig. 5a), the peak intensities of Ca 2p, O 1s and Mg 2s were significantly increased in sea water in the absence of SHMP (Fig. 5b). Qiu et al. (2016) reported that  $\text{CaMg}(\text{CO}_3)_2$  may form in pH 7~10, while  $\text{Mg}(\text{OH})_2$  and  $\text{CaCO}_3$  were formed at pH greater than 9.5 and 10, respectively. In addition,  $\text{MoS}_2$  recovery in sea water was reduced with increased pH. Therefore, these precipitates mainly contributed to the depressed flotation recovery in sea water, consistent with many previous studies reporting that the depression of sea water on sulfide flotation was mainly due to the presence of hydrophilic  $\text{Mg}(\text{OH})_2$  on minerals surface, thereby inhibiting mineral floatability (Jeldres et al., 2016; Ramos et al., 2013; Rao et al., 2016; Suyantara et al., 2018).

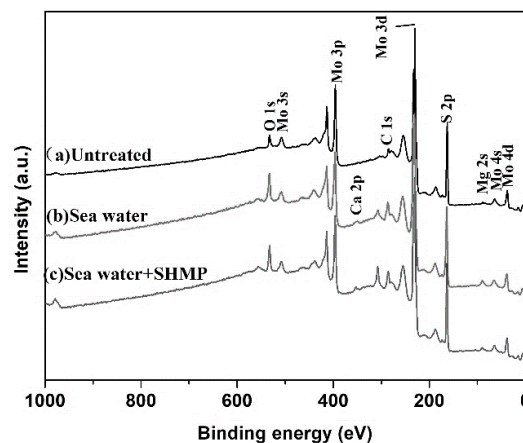


Fig. 5. XPS survey of  $\text{MoS}_2$ , (a) untreated, treated in (b) sea water and (c) sea water +SHMP at pH 10

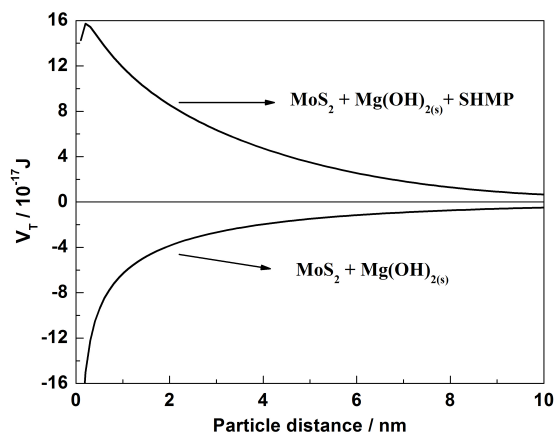
Table 1 further shows that the concentrations of O 1s, Ca 2p and Mg 2s were increased from 7% to 11%, 0 to 1% and 1% to 4%, respectively, when sea water was applied as flotation medium, suggesting that both Mg and Ca species were adsorbed onto the MoS<sub>2</sub> surface. However, Mg and O concentrations were decreased from 4% to 2%, and 11% to 7%, respectively, in the addition of SHMP, suggesting that SHMP reduced the attachments of these species on MoS<sub>2</sub> surface in sea water. The surficial species is likely Mg(OH)<sub>2</sub>, which has been reported in previous studies (Qiu et al., 2016; Ramos et al., 2013; Rebolledo et al., 2017; Suyantara et al., 2018).

Table1 Elemental quantification (at. %) of MoS<sub>2</sub>

Element	Binding Energy (eV)	Conditions		
		Untreated	Sea water	Sea water+SHMP
C 1s	284.8	6	15	15
S 2p	162.4	54	41	43
Mo 3d	230.0	32	28	32
O 1s	533.2	7	11	7
Ca 2p	351.0	0	1	1
Mg 2s	89.5	1	4	2

### 3.5. DLVO calculation

Fig. 6 shows the DLVO interaction energy between MoS<sub>2</sub> and Mg(OH)<sub>2</sub> colloids at pH 10 with and without SHMP. In the absence and presence of SHMP, the zeta potentials of Mg(OH)<sub>2</sub> at pH 10 was 11.6 mV and -23.2 mV, respectively, while the zeta potentials of MoS<sub>2</sub> was -57.5 mV and -71.9 mV, respectively. Without SHMP, the  $V_T$  between MoS<sub>2</sub> and Mg(OH)<sub>2</sub> particles was negative in the pH range examined, indicating that the attraction force was dominated between MoS<sub>2</sub> and Mg(OH)<sub>2</sub> colloids. In other words, Mg(OH)<sub>2</sub> can attach onto MoS<sub>2</sub> surfaces (Yu et al., 2018). After the addition of SHMP, the  $V_T$  was reversed from negative to positive values, suggesting that the repulsion force was dominated. This means that the precipitation of Mg(OH)<sub>2</sub> was hard to adsorb on the MoS<sub>2</sub> surface in the presence of SHMP. Therefore, the increased MoS<sub>2</sub> recovery in the presence of SHMP was mainly due to the prevention of hydrophilic Mg(OH)<sub>2</sub> precipitation attaching onto MoS<sub>2</sub> surface.

Fig. 6. Interaction energy between MoS<sub>2</sub> particles and Mg(OH)<sub>2</sub> colloids

### 4. Conclusions

The flotation recovery of MoS<sub>2</sub> in sea water was significantly reduced under alkaline condition, primarily due to the attachment of formed hydrophilic metallic species onto MoS<sub>2</sub> surface. The addition of SHMP reduced the adsorption of such precipitation. DLVO theoretical calculation demonstrated that the dominant interaction force between MoS<sub>2</sub> and Mg(OH)<sub>2</sub> colloids was attraction force, which was reversed to repulsion force in the presence of SHMP, thereby improving MoS<sub>2</sub> flotation recovery by removing Mg(OH)<sub>2</sub> from MoS<sub>2</sub> surface.

## 5. Acknowledgements

The authors gratefully thank the supports from National Natural Science Foundation of China (51604205, 51774223) and National College Students Innovation and Entrepreneurship Training Program (201810497113).

## References

- ARIAS, DAYANA., CISTERNAS, LUIS A. and RIVAS, MARIELLA., 2017. *Bio-mineralization of calcium and magnesium crystals from seawater by halotolerant bacteria isolated from Atacama Salar (Chile)*. *Desalination*. 405, 1-9.
- CASTRO, S., LOPEZ-VALDIVIESO, A. and LASKOWSKI, J. S., 2016. *Review of the flotation of molybdenite. Part I: Surface properties and floatability*. *International Journal of Mineral Processing*. 148, 48-58.
- JELDRES, RICARDO I., ARANCIBIA-BRAVO, MAR A P., REYES, ARTURO., AGUIRRE, CLAUDIA E., CORTES, LORENA. and CISTERNAS, LUIS A., 2017. *The impact of seawater with calcium and magnesium removal for the flotation of copper-molybdenum sulphide ores*. *Minerals Engineering*. 109, 10-13.
- JELDRES, RICARDO I., FORBES, LIZA. and CISTERNAS, LUIS A., 2016. *Effect of seawater on sulfide ore flotation: a review*. *Mineral Processing & Extractive Metallurgy Review*. 37, 369-384.
- LAZGHAB, MARIEM., SALEH, KHASHAYAR., PEZRON, ISABELLE., GUIGON, PIERRE. and KOMUNJER, LJEPSA., 2005. *Wettability assessment of finely divided solids*. *Powder Technology*. 157, 79-91.
- LI, W., LI, Y., XIAO, Q., WEI, Z. and SONG, S., 2018. *The Influencing Mechanisms of Sodium Hexametaphosphate on Chalcopyrite Flotation in the Presence of MgCl<sub>2</sub> and CaCl<sub>2</sub>*. *Minerals*. 8, 150-168.
- LI, W. and LI, Y., 2019. *Improved understanding of chalcopyrite flotation in seawater using sodium hexametaphosphate*. *Minerals Engineering*. 134, 269-274.
- LI, W., LI, Y., WEI, Z., XIAO, Q. and SONG, S., 2018. *Fundamental Studies of SHMP in Reducing Negative Effects of Divalent Ions on Molybdenite Flotation*. *Minerals*. 8, 404-421.
- LI, Y., CLEMENT, L., SONG, S., LI, Y. and GERSON, A. R., 2018. *The fundamental roles of monovalent and divalent cations with sulfates on molybdenite flotation in the absence of flotation reagents*. *RSC ADVANCES*. 8, 23364-23371.
- LI, Y., LI, W., WEI, Z., XIAO, Q., CLEMENT, L., LI, Y. and SONG, S., 2018. *The Influence of Common Chlorides on the Adsorption of SBX on Chalcopyrite Surface during Flotation Process*. *Mineral Processing and Extractive Metallurgy Review*. 1-12.
- LI, Z., HAN, Y., LI, Y. and GAO, P., 2017. *Effect of serpentine and sodium hexametaphosphate on ascharite flotation*. *Transactions of Nonferrous Metals Society of China*. 27, 1841-1848.
- LIU, G., LU Y., ZHONG, H., CAO, Z. and XU, Z., 2012. *A novel approach for preferential flotation recovery of molybdenite from a porphyry copper-molybdenum ore*. *Minerals Engineering*. 36-38, 37-44.
- LU, J., SUN, M., YUAN, Z., QI, S., TONG, Z., LI, L. and MENG, Q., 2019. *Innovative insight for sodium hexametaphosphate interaction with serpentine*. *Colloids Surf Physicochem Eng Aspects*. 560, 35-41.
- LUIS, A, CISTERNAS, G LVEZ., EDELMIRA, A. and LOPEZ-VALDIVIESO., 2015. *Study of the natural floatability of molybdenite fines in saline solutions and effect of gypsum precipitation*. *Minerals and Metallurgical Processing*. 32, 203-208.
- QIU, Z., LIU, G., LIU, Q. and ZHONG, H., 2016. *Understanding the roles of high salinity in inhibiting the molybdenite flotation*. *Colloids and Surfaces A: Physicochemical and Engineering Aspects*. 509, 123-129.
- RAMOS, O., CASTRO, S. and LASKOWSKI, J. S., 2013. *Copper-molybdenum ores flotation in sea water: Floatability and frothability*. *Minerals Engineering*. 53, 108-112.
- RAO, F., L ZARO, I. and IBARRA, L. A., 2016. *Solution chemistry of sulphide mineral flotation in recycled water and sea water: a review*. *Mineral Processing and Extractive Metallurgy*. 126, 139-145.
- REBOLLEDO, ERICK., LASKOWSKI, JANUSZ S., GUTIERREZ, LEOPOLDO. and CASTRO, SERGIO., 2017. *Use of dispersants in flotation of molybdenite in seawater*. *Minerals Engineering*. 100, 71-74.
- SUYANTARA, GDE PANDHE WISNU., HIRAJIMA, TSUYOSHI., MIKI, HAJIME. and SASAKI, KEIKO., 2018. *Floatability of molybdenite and chalcopyrite in artificial seawater*. *Minerals Engineering*. 115, 117-130.
- WANG, B., PENG, Y., 2014. *The effect of saline water on mineral flotation – a critical review*. *Minerals Engineering*. 66-68, 13-24.
- LI, Y., LI, W., XIAO, Q., HE, N., REN, Z., CLEMENT, L. and GERSON, A. R., 2017. *The Influence of Common Monovalent and Divalent Chlorides on Chalcopyrite Flotation*. *Minerals*. 7, 111-121.
- XIA, W., 2017. *Role of surface roughness in the attachment time between air bubble and flat ultra-low-ash coal surface*. *International Journal of Mineral Processing*. 168, 19-24.

YU, Y., MA, L., XU, H., SUN, X., ZHANG, Z. and YE, G., 2018. *DLVO theoretical analyses between montmorillonite and fine coal under different pH and divalent cations*. Powder Technology. 330, 147-151.